Hindawi Publishing Corporation
Advances in Materials Science and Engineering
Volume 2009, Article ID 254848, 11 pages
doi:10.1155/2009/254848

Research Article

Plasma Spraying and Characterization of Tungsten Carbide-Cobalt Coatings by the Water-Stabilized System WSP

Pavel Ctibor,[1] Micheala Kašparová,[2] Jeremy Bellin,[3] Emmanuel Le Guen,[3] and František Zahálka[2]

[1] *Institute of Plasma Physics ASCR, Za Slovankou 3, 182 00, Praha 8, Czech Republic*
[2] *Skoda Research Ltd., Tylova 57, 316 00 Plzeň, Czech Republic*
[3] *Engineering National School of Limoges, 16 rue Atlantis, 87068 Limoges, France*

Correspondence should be addressed to Pavel Ctibor, ctibor@ipp.cas.cz

Received 17 June 2009; Revised 19 October 2009; Accepted 19 October 2009

Recommended by Jenn-Ming Yang

Tungsten carbide-cobalt powders (WC-17wt% Co) were plasma sprayed by a water-stabilized system WSP. Experiments with variable feeding distances and spray distances were carried out. Thinner coatings were deposited on carbon steel substrates and thicker coatings on stainless steel substrates to compare different cooling conditions. Basic characterization of coatings was done by XRD, SEM, and light microscopy plus image analysis. Microhardness was measured on polished cross-sections. The main focus of investigation was resistance against wear in dry as well as wet conditions. The appropriate tests were performed with set-ups based on ASTM G65 and G75, respectively. The influence of spray parameters onto coating wear performance was observed. The results of mechanical tests were discussed in connection with changes of phase composition and with the quality of the coating's microstructure. The results show that for obtaining the best possible WC-17Co coating with WSP process, from the viewpoint of wear resistance, the desired parameters combination is long feeding distance combined with short spray distance.

1. Introduction

Tungsten carbide-cobalt (WC-Co) based materials are used extensively in industry in their sintered as well as thermally sprayed forms for applications requiring abrasion, sliding, fretting, and erosion resistance. The hard WC particles form the major wear-resistant constituent of these materials, while the cobalt binder provides toughness and cohesion. Properties such as hardness, wear resistance, and strength are influenced primarily by the WC grain size and volume fraction and, with thermally sprayed coatings, also by varying the porosity and (often unintentionally) the carbide and binder phase composition [1].

The bulk processing route can be costly and is limited to the production of relatively small components. Fortunately, however, for many wear applications, it is only the contact surface properties that are important in determining the wear resistance of the components. Therefore, the use of a coating technique, such as thermal spraying, has several attractive features for producing wear-resistant components [2].

WC contains 6.13% C and has a microhardness of about 24 GPa, while W_2C contains 3.16% C and has a microhardness of about 30 GPa, but is more brittle than WC [1]. Despite the fact that W_2C is metastable below 1250°C, it is often present in WC-Co, even after slow cooling. The metastable phase γ or WC_{1-x}, however, is found only at room temperature when the material has been quenched rapidly. WC-Co is therefore a difficult material to successfully process in the extremely high-temperature, oxidizing/decarburizing conditions generated during thermal spraying, particularly plasma spraying [1].

In plasma spraying, the WC-Co powder tends to undergo a combination of decarburization, oxidation, reduction by reaction with the H_2 in the plasma gas, and dissolution/reaction between the WC and the cobalt binder metal

during spraying, all resulting in the formation of hard and brittle phases such as W_2C, $Co_xW_yC_z$, and even WO_3 and W [1].

The decarburization of a powder particle is expected to proceed as follows [3]. The cobalt will melt and WC will dissolve into the liquid as the temperature rises. Carbon will be removed from the melt either by reaction with oxygen at the melt/gas interface or through oxygen diffusion into the rim of the molten particle, leading to a carbon monoxide formation. The depletion of carbon from the melt will thus be restricted to a shell region, the depth of which will depend on transport of carbon, oxygen, and the reaction kinetics. However, removal of carbon, locally, from the melt will drive further dissolution of WC grains in this shell region as the system attempts to re-establish local equilibrium at the WC-melt interface.

The decarburization itself is associated also with dissolution of W and C in the Co matrix. As a WC–Co powder particle enters the hot gas its temperature increases and the Co phase will begin to melt (pure Co melts at 1495°C) after a relatively short time [3]. Once the Co is molten WC will begin to rapidly dissolve in it and at 1500°C approximately 30 wt% W and 2.5 wt% C can dissolve. Furthermore, as a particle's temperature continues to increase, more WC will dissolve. At 2000°C molten Co in equilibrium with WC could contain 50–60 wt% W and 3–3.5 wt% C.

The principal resulting microstructural features are [3]. (i) the reduction in volume fraction of the carbide in the coating compared with the powder; (ii) the formation of an amorphous or nanocrystalline binder phase; (iii) the formation of two distinct regions of the binder phase, one being significantly richer in tungsten than the other; (iv) the formation of W_2C and W; W_2C is often observed to encapsulate WC grains; (v) the reduction in carbon content of the coating compared with the powder.

The above-mentioned hypothesis was based on a study of HVOF coatings. In the case of atmospheric plasma spraying, the higher the enthalpy of the plasma gas, the more WC decarburization and reaction with the binder phase can be expected, because more thermal energy is available to drive the process [1]. This danger is especially high in the case of the water stabilized plasma gun WSP, which has high plasma enthalpy and exit temperature [4].

The presence of oxygen in APS is also believed to promote the nucleation of oxy-carbides [5] in a considerable amount, which is undesirable for wear resistance. Decarburization of WC was markedly reduced during the plasma spray process using Ni-coated particles surface [6–8]. Furthermore, the two main differences between cobalt and nickel binder phases are that (i) nickel is considerably more corrosion resistant than cobalt and (ii) it is a stable f.c.c. structure and hence does not undergo a phase transformation [7].

It should be noted that the decarburization degree of detonation gun-sprayed WC-Co coating is much lower than that by other thermal spraying techniques [5]. The HVOF technique is usually considered to be the best one for WC-Co spraying [1, 9, 10]. However, besides thermal and quenching stresses, residual stresses in HVOF coatings could also be due to peening stresses produced due to the kinetic energy of the impinging particles with the substrate or previously deposited material [11]. This phenomenon is not so dangerous in plasma spraying with significantly lower particle velocities. However, in majority of cases the influence of the peening stress is not so strong to make HVOF less prospective than plasma spraying.

It may be observed that cobalt is not often detected by XRD [1]. Partly the reason is that significantly large amounts of amorphous phases are present in plasma sprayed coatings.

Abrasion wear resistance of WC-based cermets is in a first order of magnitude a function of the hardness of a surface and the cohesion of the spray particles in the layer [6]. Agglomerated powders are sometimes used for the decrease of spallation [12], which is also associated with brittleness of certain structural components. Laser cladding of WC-Ni composite was tested [13] for wear application. Microhardness 1150 $HV_{0.3}$ (i.e., 11.5 GPa) is reported for coating produced by detonation gun spraying [14], 11 to 13 GPa for plasma sprayed samples [12] and in the same frames for HVOF [9, 10]; whereas 11 to 16 GPa are values of HVOF thermally posttreated coatings [10].

The goal of this work was to study phenomena taking place during spraying of WC-based powders by WSP device and to characterize the resulting coatings. WC-17 wt%Co materials were the main object of investigation; however, WC-8 wt%Co was also sprayed together with a mechanical mixture of WC and Ni as well, to receive a more complete insight into the WC-based cermets behavior at the WSP process.

2. Experimental

2.1. Powders and Spraying. The powder WC-17 wt%Co was obtained as a commercial product—(label PT-73PTA-40, Plasmatec, Montreal, Canada). The nominal size of this powder was from 100 to 140 μm. The powder WC-8 wt%Co was obtained as a laboratory product—(SVUM, Czech Republic). The nominal size of this powder was from 63 to 90 μm. The powder WC-17 wt%Ni was prepared at the Institute of Plasma Physics (IPP), by mechanical mixing of commercial WC and Ni powders. The WC powder exhibited the size 40 to 80 μm (Alldyne, AL, USA) and Ni powder the size 100 to 140 μm (SVUM, Czech Republic).

Spraying was carried out by a water-stabilized plasma gun WSP 500 at IPP. WSP system utilizes water instead of gas to produce thermal plasma. Water vortex is created in a plasma-forming chamber around the electric arc burning between consumable graphite cathode and rotating external anode. This design dictates an external feeding. Also the distance between the plasma exit nozzle and the point where powder feedstock is fed in is called "feeding distance;" whereas the distance from the nozzle to a substrate is called "spray distance." Table 1 summarizes conditions specific for all samples; abbreviations FD for feeding distance and SD for spray distance are used. Arc power was 153.6 kW (given by current 480 A and voltage 320 V); feed rate 15 kg/h (i.e., 250 g/min); powder injection angle 60°—all were used as a setup parameters for majority of experiments, exceptions

Table 1: Samples of WC-based coatings.

Sample label	Coating material	Substrate material	FD [mm]	SD [mm]	Exceptional conditions
a	WC-17Co	SS	70	350	—
b	WC-17Co	SS	85	350	—
c	WC-17Co	SS	100	350	—
d	WC-17Co	SS	70	450	—
e	WC-17Co	SS	85	450	—
f	WC-17Co	SS	100	450	—
aa	*WC-17Co*	*CS*	*70*	*350*	—
bb	*WC-17Co*	*CS*	*85*	*350*	—
cc	*WC-17Co*	*CS*	*100*	*350*	—
dd	*WC-17Co*	*CS*	*70*	*450*	—
ee	*WC-17Co*	*CS*	*85*	*450*	—
ff	*WC-17Co*	*CS*	*100*	*450*	—
g	WC-17Ni	SS	100	450	Feed rate 18 kg/h
h	WC-8Co	*CS*	(35)	350	Feed rate 12 kg/h
i	WC-17Co	SS	115	350	—
j	WC-17Co	SS	115	300	—

are indicated in Table 1. Powder was fed into the plasma jet by two injectors and forced in by Ar gas with flow rate 3.2 slpm. Substrates were preheated to 180°C in all cases. Thinner coatings (0.2 mm) were carried out on carbon steel ("CS" in Table 1) substrates and thicker coatings (0.6 mm) on stainless steel ("SS" in Table 1) substrates in order to compare faster cooling conditions—the former case—with slower cooling conditions. The cooling speed is low for thick WC-based coating on low-conductivity stainless steel (with thermal conductivity approximatly 4 times lower than carbon steel). All substrates were grit blasted before spraying. The maximum temperature measured during spraying was 160°C in the case of carbon steel substrates and 310°C in the case of stainless steel substrates. The example of a temperature evolution at spraying of WC-8Co is given on Figure 1.

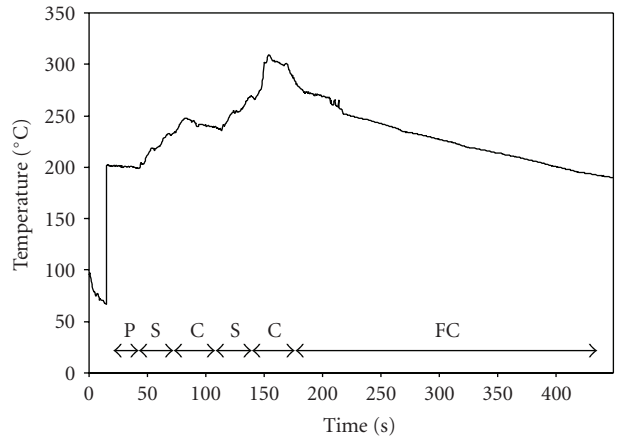

Figure 1: Temperature evolution at spraying of WC-8Co. P: preheating; S: spraying; C: cooling (by compressed Ar); FC: "fine" cooling (by compressed Ar with reduced flow rate). The signal was collected from a thermocouple screwed on the substrate backside.

2.2. Characterization Techniques. Powder size distribution was determined by the laser scattering device Analysette 22 (Fritsch, Germany) in H_2O + $Na_4P_2O_7$. Scanning electron microscope Camscan 4 DV (Camscan, UK) and light microscope Neophot 32 equipped by a CCD camera were used for structural investigation. X-rays diffractometer D 500 (Siemens AG, Germany) with filtered Cu radiation was used for phase analysis. Angle 2 theta from 10 to 90° was recorded with step 0.02°. Surface roughness was determined by the apparatus Surtronic 3P (Taylor Hobson, UK). Path length 25 mm was used on 5 different tracks, as parameters describing the surface R_a and R_{ymax} were selected.

Porosity was studied by the light microscopy on polished cross sections. Micrographs were taken with a CCD camera and processed using the image analysis (IA) software (Lucia G, Laboratory Imaging, Prague, Czech Republic). A minimum of 10 images of microstructures, taken from various areas of a cross section for each sample, was analyzed. The magnification used was 250 in all cases allowing an analysis into all objects with size of 3 microns or more. For a better description of the size distribution of free flight particles (FFP), collected by placement of Ar-filled container instead of a substrate, certain additional criteria were introduced.

(i) "Equivalent diameter" (ED) represents their size distribution (approximation at 2D projection).

(ii) "Circularity" (CIR) describes the shape of particles when "1" represents a perfect circle and "0" the linear projection; it is calculated for at least 10 images. "Maximal CIR" (CIR_{max}) is then a parameter used for distinction between samples; small CIR_{max} indicates rather elongated shapes while high CIR_{max} characterizes good spheroidization of FFP.

Microhardness was measured by the Hanemann microhardness head mounted on the light microscope with fixed load 1 N and the Vickers indenter on a microhardness head (Carl Zeiss, Germany) attached to the light microscope Neophot 2. Twenty indentations from various areas of a cross section for each sample were analyzed.

Slurry abrasion response of coatings (SAR test) was measured according to a modified ASTM G-75 test [15]. Main modification contains the fact that ASTM emphasizes the use of a reference sample, which is a bulk alloy—targeted to comparison with bulk metals and not with cermet coatings. The authors of this paper are using successfully the SAR test without the ASTM reference samples [16–18]. The applied force was 22.24 N per specimen and alumina particles mixed with water served as the abrasive slurry. The test represents a 9216 meters path divided into four increments with mass loss being measured at the end of each 2304 m increment, when the specimens were ultrasonically cleaned and weighed. Accuracy of the measurement is about ±5%.

Besides basic SAR test also a response of samples onto various abrasive medium particle sizes was tested. Two different sizes of alumina abrasive powder were used. The first series of tests was made in finer powder "P1" (20 to 80 microns) and the second series in coarser powder "P2" (10 to 125 microns). The second powder, however being of nominally smaller mean size, contains larger particles (over 100 μm), which are important for the wear action.

Selected samples were tested also in slurry containing garnet powder with size from 400 to 950 μm, dedicated to grit blasting. The main reason for the selected sizes was the fact that the fine powder particles are smaller than the splat size of the coating with reference to both alumina powders P1 and P2; whereas particles are significantly larger than splats regarding garnet powder P3. Alumina powder in size comparable to P3 is however too aggressive to receive well detectable results especially for relatively thin coatings; this was the reason for preferring slightly weaker garnet powder.

The dry rubber wheel (traditionally called Dry Sand - Rubber Wheel; DSRW) abrasion test, a modified version of ASTM G-65 [19], was performed using alumina particles as the abrasive. The modifications of the ASTM prescriptions, were, namely, in the abrasive particle size and rubber type (hardness). The abrasive was fed between the coated sample and the rotating rubber wheel. The particle size of the alumina powder was 212–250 μm and the samples were pressed against the rubber wheel with the force of 22 N. The test comprises 2000 revolutions of the wheel, which corresponds to a wear length of 1436 m. All the coating weight losses were transformed to volume losses by applying densities measured by the Archimedean method—roughly 13.1 g/cm^3. Accuracy of the measurement is approximatly ±8%.

3. Results and Discussion

3.1. Powder before and after Flight in Plasma Jet. Size distribution of the WC-17Co powder used for majority of experiments is displayed in Figure 2 together with the microphotograph. The powder production route was sintering with subsequent crushing, which produces the nonconvex surface and also elongated shape. The nominal size of this powder was from 100 to 140 μm, but according to Figure 2(a) (see the histogram) a certain amount of the particles up to 200 μm is present. Moreover some particles are elongated (Figure 2(b)) and therefore their real size is markedly larger than the corresponding mesh size.

Image analysis of the free-flight particles (FFPs) has revealed substantial melting of FFP manifesting itself in spherical shape of solidified droplets. The spheroidization is detected by IA on 2D projections as circularity (see Figure 3(a)). We can see a significant increase of CIR_{max} for all FD in comparison with the feedstock (feedstock is represented by FD "0"). The difference between samples sprayed with various FD is negligible. The size reduction of the particles in plasma was about 10 percent, based on IA results (parameter ED). Also, in-flight evaporation would not take place.

3.2. Coatings—Structure. For industrial applications, good quality, coherent, and well adherent coatings are desirable. Such a combination of properties was not achieved by our spray tests in spite of obtaining lot of information about behavior of WC-based materials during WSP process.

The sintered and crushed powders are reported to contain typically WC grains having size 2 to 5 μm [3] or elsewhere 5 to 7 μm [1]. Coatings produced using sintered and crushed powder are reported to contain WC particles size 1 to 2 μm (sometimes up to 4 μm). This implies either a genuine loss of carbide during spraying or the breakup of the larger apparent WC grains into the smaller [1]. Our coatings exhibit the same WC grain size as used feedstocks, that is, between 2 and 8 μm; see Figure 4.

In the darker (i.e., cobalt-rich [3]) matrix on our cross sections (Figure 4), lighter, blocky, angular particles, presumably of WC, have been identified. The corresponding volume fraction of carbide phase (based on IA—area fraction measurements) within the coating was 69 to 78%.

The X-ray diffraction pattern of WC-17Co coatings is given in Figure 5. The combination of spray parameters 35–350 was chosen because of the large feedstock powder size (the discrepancy between the nominal and real maximum sizes has been discussed above). The motivation of using as short FD as 35 mm was to enhance the melting of even the largest particles. But this coating exhibited very low cohesion and was not able to withstand slurry testing and also metallographic preparation. Therefore the coatings with FD 35 mm were excluded from mechanical testing. In Figure 5 the sample FD 35 exhibits also the strongest decarburization manifesting itself in high W_2C peaks intensity. Other two coatings in Figure 5 exhibit similar diffraction patterns with a hump, centered at approximatly 42°, which according the literature [3, 20] corresponds to amorphous fraction. Besides WC and W_2C, also WO_3 and $CoWO_4$ phases were detected. Complex carbides are represented with η-phase (Co_6W_6C) and certain peaks correspond also to elemental tungsten and

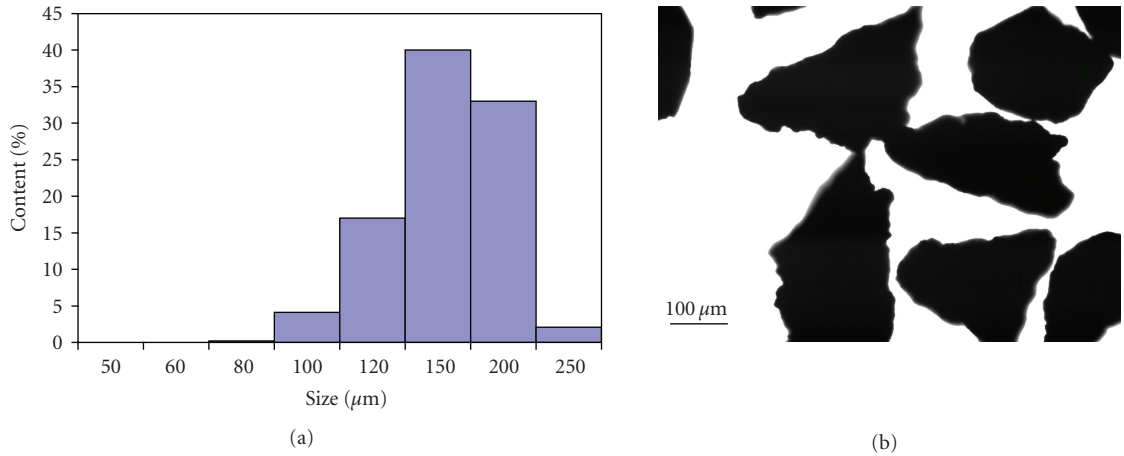

(a) (b)

Figure 2: (a) Size distribution of the powder WC-17Co. (b) Microimage of the powder WC-17Co; light microscopy in transmitted light.

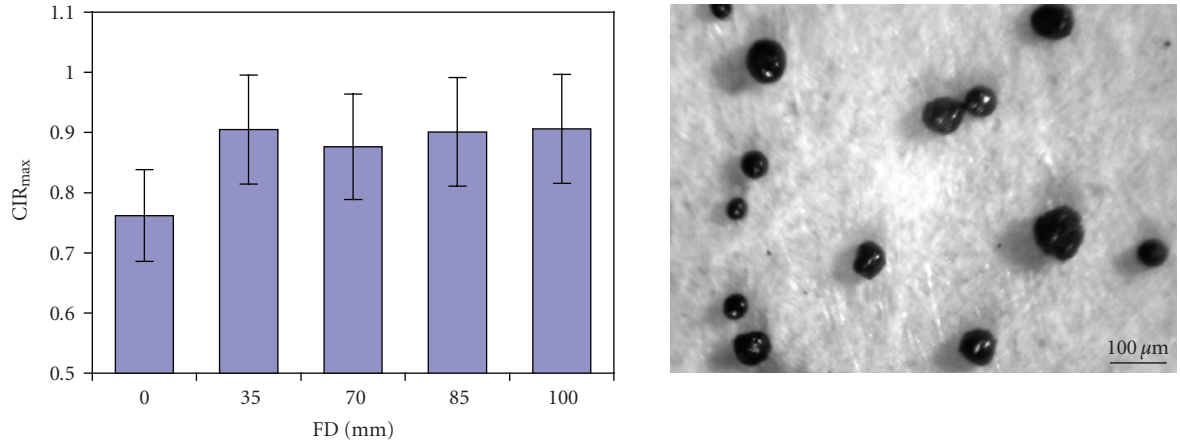

(a) (b)

Figure 3: (a) Circularity of free-flight particles of WC-17Co. (b) Microimage of free-flight particles; light microscopy in reflected light.

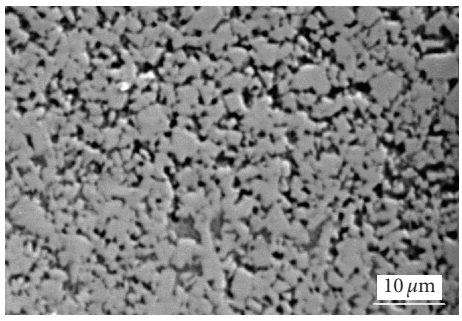

Figure 4: Microstructure of the optimized coating FD 115-SD 300; SEM.

carbon (graphite). The peak indicated by "y" could belong to WO_2 or η-phase or η_2-phase (Co_3W_3C). There are no very pronounced differences between coating sprayed from FD 70 and FD 85, the only significant change is in more easily detectable WO_3 at FD 85. The powder fed in the plasma jet at higher FD penetrated into plasma mixed more intensively with surrounding air due to turbulent flow, also this zone is richer in oxygen, responsible at certain conditions for in-flight oxidation.

X-ray diffraction pattern of WC-17Co coating sprayed with FD 115 mm and SD 300 mm is given on Figure 6. The character of the pattern and main detected components do not differ markedly from FD 70 and FD 85, only the (001) peak of WC is less intensive at 115–300 coating. Presence of W_2C as well as complex carbides was confirmed.

X-ray diffraction pattern of WC-17Ni coating (sprayed with FD 100 mm and SD 450 mm) is given on Figure 7. W_2C main peak has high intensity and WC can be also detected; however its relative quantity seems to be lower then at WC-Co coatings. Oxides of both metals, W (i.e., WO_3) and Ni (i.e., NiO), and also elemental metals are present. The peak indicated by "y" could belong to WO_2.

All WSP sprayed WC-based coatings are rather porous, see Figure 8, despite whether substrate was well thermally conductive (carbon steel) or less thermally conductive (stainless steel). The porosity as detected by IA varies between 14

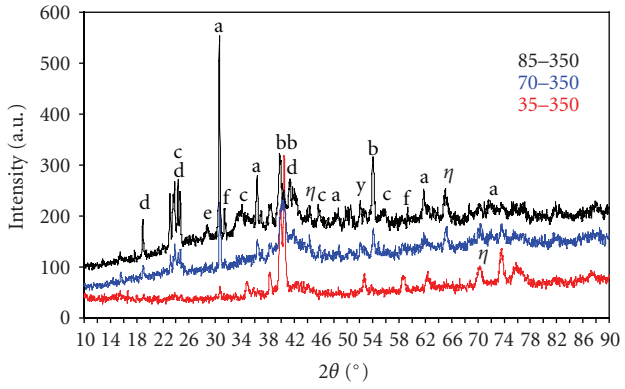

a WC
b W_2C
c WO_3
d $CoWO_4$
e Graphite
f Tungsten
η Co_6W_6C
y Co

Figure 5: X-ray diffraction pattern of WC-17Co coatings sprayed with SD 350 mm.

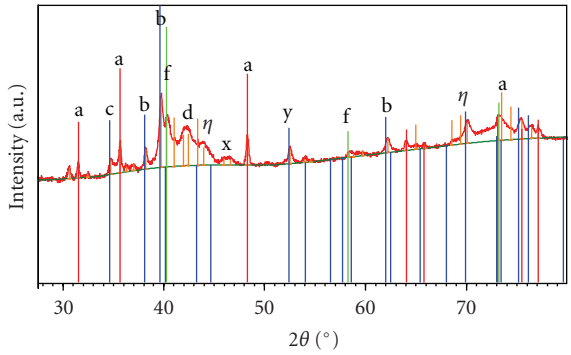

a WC
b W_2C
c WO_3
d $CoWO_4$
f Tungsten
η Co_6W_6C
y Co

Figure 6: X-ray diffraction pattern of WC-17Co coating sprayed with FD 115 mm and SD 300 mm.

and 24% including WC-8Co samples and WC-Ni samples. The general trends were that smaller SD leads to slightly higher porosity, but the pores are smaller, more globular, and less interconnected, which is advantageous for coating integrity influencing the wear resistance.

Ni-coated WC coatings were used for a limitation of the occurrence carbon-deficient phases in plasma sprayed coatings [21]. Our XRD results confirm this trend only partly (because Ni was not coated on the WC surface in the feedstock) but there is not presence of complex carbides like in the case of Co binder. These carbides are favorable for hardness improvement but due to their brittleness are problematic from the wear resistance viewpoint. Oxy-carbides were not detected in our coatings regardless feedstock composition (Ni or Co binder). It has to be noticed that the price of the feedstock is markedly lower in the case of WC-Ni, prepared as described above, compare to WC-Co

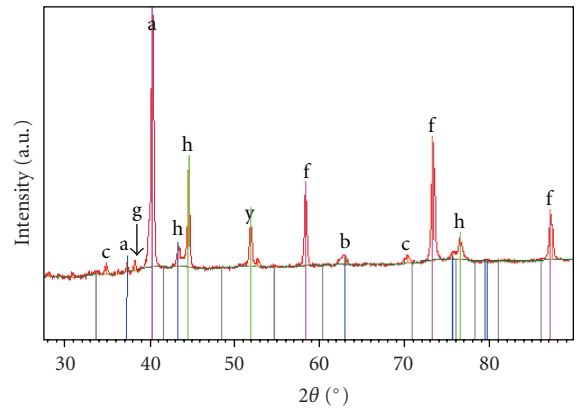

a WC
b W_2C
c WO_3
f Tungsten
g NiO
h Ni
y Co

Figure 7: X-ray diffraction pattern of WC-17Ni coating.

powder. This one was tailored by the producer for us from the size viewpoint; WSP needs coarser feedstock than other plasma guns as a consequence of its thermal and electrical characteristics. Other consequences of the use of our WC-Ni are discussed in Section 3.3.1.

3.3. Coatings—Properties

3.3.1. Surface Properties, Microhardness, and Wear Resistance. Surface roughness of WC-based coatings is summarized in Table 2. Sample WC-8Co has the lowest roughness, which was caused by using finer feedstock than WC-17Co. WC-Ni coating, however, sprayed from bimodal-size feedstock, has roughness comparable with WC-17Co coatings (a)–(f). The surface of WC-Ni coating is visualized in a three-dimensional image, Figure 9. Surface roughness of WC-17Co coatings sprayed using FD 115 is however even larger.

Microhardness (Figure 10) of WC-17Co coatings (a)–(f) is above 12 GPa, and the value of WC-8Co coating is only slightly below it. On the contrary, the value of WC-Ni coating is as low as 5.5 GPa, that is, less than 50% of WC-Co coatings. The high hardness of WC-Co coatings seems to be due to the W_2C phase and complex carbides; whereas the lower hardness is due to the absence of complex carbides in WC-Ni coating and presence of metal elements.

The microhardness is the highest for WC-17Co coating with FD 115 mm. The dominance of W_2C over WC is most pronounced in these coatings.

Dry and wet abrasion test results are expressed in Figure 11 as a wear coefficient in C_w [mm^3/Nm] for easy comparison of both techniques. Lower C_w indicates better wear resistance. We see that WC-17Co samples sprayed using shorter SD (350 mm) have a similar C_w at the SAR and DSRW test. On the other hand, samples sprayed using longer SD (450 mm) have at DSRW approximately twice higher C_w than that at the SAR test. This interesting fact is probably associated with the coating cohesion and

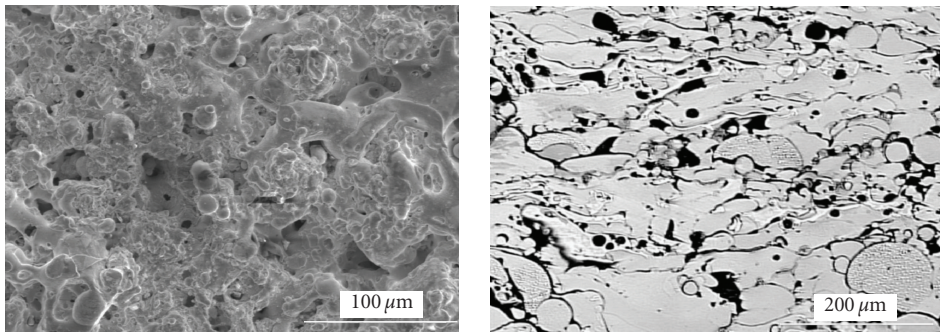

(a) (b)

Figure 8: (a) Surface of as-sprayed WC-17Co coating 85–350; SEM. (b) Cross section of 85–350; light microscopy.

Table 2: Surface roughness of WC-based coatings.

Sample	R_a [μm]	St. Dev. [μm]	R_{ymax} [μm]	Std. Dev. [μm]
WC-17Co 70–350	18.3	0.8	137.2	11.8
WC-17Co 70–450	14.5	0.5	120.7	10.6
WC-17Co 85–350	16.9	0.9	132.7	16.2
WC-17Co 85–450	13.5	2.1	116.4	18.9
WC-17Co 100–350	15.5	1.1	115.5	15.5
WC-17Co 100–450	15.3	0.7	116.6	12.9
WC-8Co	9.4	0.6	70.0	3.8
WC-Ni	15.2	0.5	108.7	9.5
WC-17Co 115–350	29.2	3.9	183.9	25.9
WC-17Co 115–300	26.1	1.0	167.0	16.4

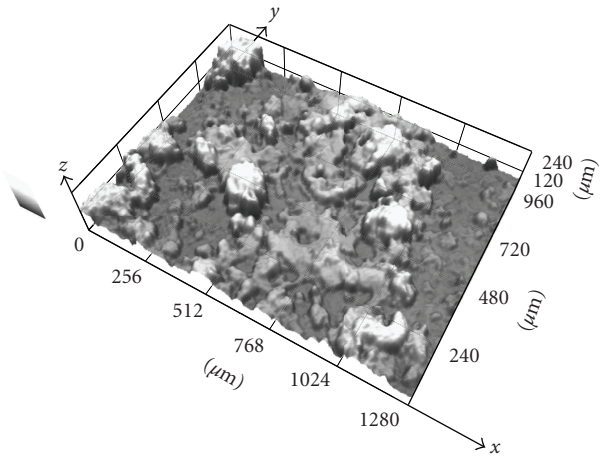

Figure 9: Reconstructed 3D of WC-Ni coating as-sprayed surface; laser confocal microscopy.

degree of interlamellar bonding, which usually decreases with increasing SD.

WC-Ni coating has DSRW and also SAR wear resistance fully comparable with WC-Co (a)–(f), despite dramatically lower hardness. Our WC-Ni coating regardless of its lower price could compete with some of our WC-Co in wear resistance, also this can possibly offer an interesting alternative. WC-8Co coating has a slightly higher wear coefficient at the SAR test than (a)–(f) WC-17Co coatings. The small thickness of this coating precluded performing the DSRW test.

3.3.2. Wear Mechanisms and Worn Surface Character, Sensitivity on Abrasive Agent Size. Typical examples of wear surfaces after wet (SAR) abrasion are shown in Figure 12. Chipping as a wear mechanism was less pronounced in the case of wet abrasion than at dry abrasion, similarly to [22]. The WC grains surface became worn by micropolishing. Fragments of grains also fell off from the coating surface. The main reason of it could be seen in the fact that at dry abrasion (DSRW) the velocity of the sample versus the abrasive particles is markedly higher—nearly one order of magnitude (176 m/min versus 18 m/min). At high velocities the temperature at the contact surface grows, the material could exhibit certain signs of plastic deformation [23] instead of brittle fractioning.

The mechanism of wear at the DSRW test is similar for all cermet coatings. The worn surface is smooth, with very shallow irregular grooves. The hard carbide particles protect the coatings against deep penetration of abrasive particles and lower the free path of groove. The major mechanism of wear is connected with removing the matrix from the areas between coatings' hard particles, followed by weakening of their attachment and pulling off from the coating surface—see Figure 12(c).

At the SAR test the abrasive medium is conformable to a medium used for grinding in the process of metallographic

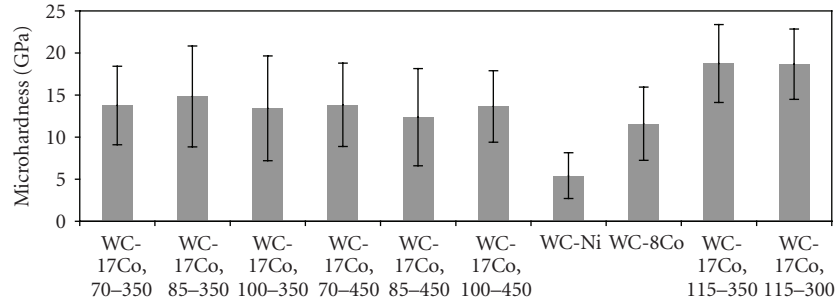

Figure 10: Microhardness of various WC-based coatings.

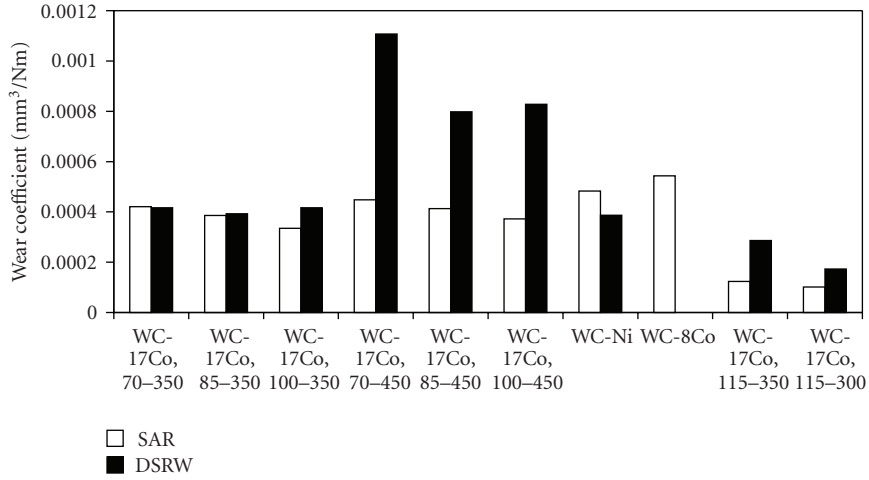

Figure 11: Results of the wet (SAR) and the dry (DSRW) abrasion tests.

sample preparation. Also the wear mechanism of cermet coatings can be described as microgrinding and polishing of coatings material. The material loss is observed preferably in the matrix, but the shape of hard carbides changed from sharp-edged to more ground. The appearance of worn surface is the same for all WC-based cermet coatings (Figure 12(b)). It was demonstrated that if the SAR powder size is changed but it remains (powders P1 and P2) in frames given by the WC phase grain size (as minimum, i.e., approximatly 10 μm) and the splat diameter in the spray direction (as maximum, i.e., approximatly 200 μm), the response of the coatings produced with different spray parameters does not differ dramatically. On the contrary, when the SAR powder size is larger than the splat diameter in the spray direction (P3 powder), strong difference occurs. As seen in Figure 13(b), coatings sprayed with shorter SD are markedly more resistant to coarse SAR powder; whereas coatings sprayed with longer SD exhibit higher wear. This fact could be associated with poor bonding of splats in coatings sprayed with longer SD. However, also the coating 100–350, having good resistance to wear in coarse powder P3 (see Figure 13(b)), looks differently after the SAR test in fine powder P1 and coarse powder P3 (see Figure 12). After a test with coarser powder, deeper craters occur on the surface and opening of the pores takes place. Roughness measurement confirmed the smoother character of surface worn by finer abrasive powder.

3.3.3. Substrate Type, Coating Thickness, and Wear Resistance. Figure 14 shows DSRW results of samples sprayed by the same parameters, that is, SD fixed at 350 mm and FD varied at 70, 85, and 100 mm on different substrates (cf. Table 1). For each FD the thicker coating on a less thermally conductive substrate is more wear resistant then the thinner one on a highly conductive substrate. The conditions for splat formation are better, when the heat withdrawal at the substrate surface decreases [24], and the corresponding coating is more wear resistant. Moreover we see a trend of increasing the difference between both thickness/substrate types with increasing FD. Long FD at fixed SD means a shorter dwell time than a short FD and a correspondingly larger influence of substrate conditions. So at the longest FD the effect of slow cooling after splat formation is mostly pronounced and thin coating formed at this FD on carbon steel is markedly less wear resistant than the thicker coating on stainless steel. High SD means colder particles at impact and hence typically lower quenching stress. The level of quenching stress is also

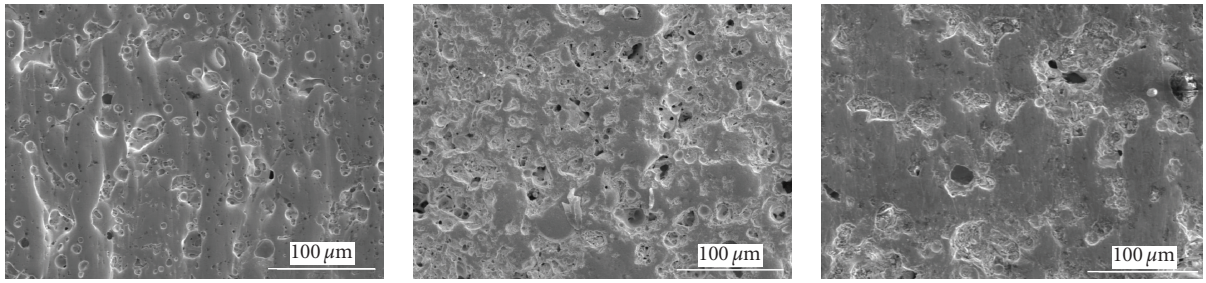

(a) (b) (c)

Figure 12: (a) WC-17Co coating 100–350 after SAR test in alumina powder P1. (b) WC-17Co coating 100–350 after SAR test in garnet powder P3. (c) WC-17Co coating 100–350 after DSRW test.

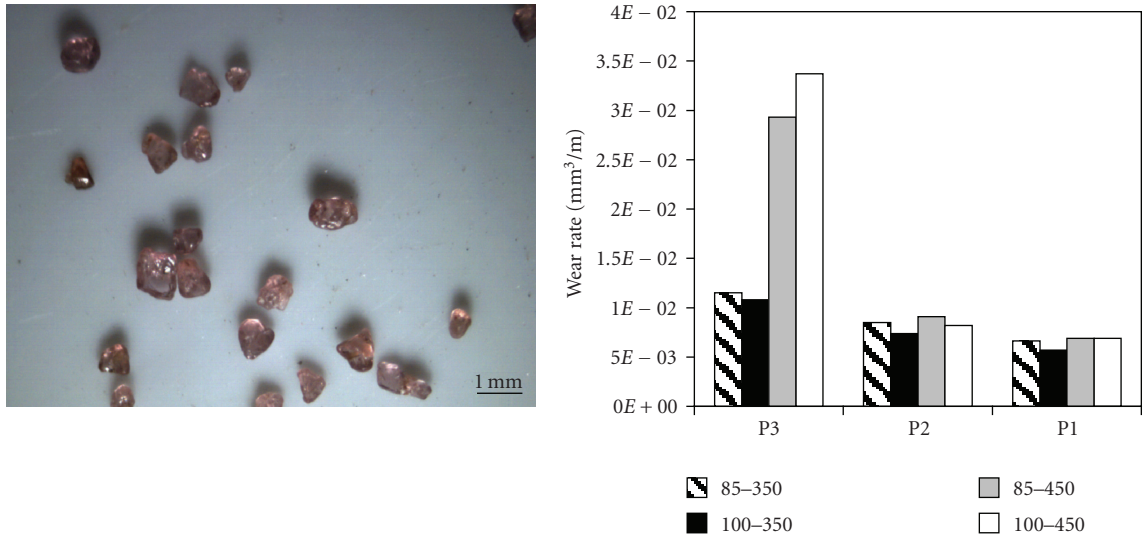

(a) (b)

Figure 13: (a) Microimage of the garnet powder; light microscopy in reflected light. (b) SAR results of WC-17Co coatings in the garnet powder P3 compare to P2 and P1.

a factor influencing the wear resistance. However in the case of our WSP coatings, probably due to high porosity, all above discussed trends seem to show that the influence of coating cohesion is more important than the influence of residual stress.

In Table 3 we could compare the principal investigated parameters for the WC-17Co (115–300) coating selected as the best one with HVOF sprayed coating of this material and also with WSP plasma sprayed Cr_2O_3 and electroplated hard chrome. All tests were done by the authors with the same techniques. We see that WSP sprayed coating WC-Co (115–300) is the hardest one. At the same time it has better dry abrasion (DSRW) than chromium oxide coating and hard chrome, but about 2 times worse than HVOF sprayed WC-Co coating. Wet abrasion (SAR) of this 115–300 coating is similar as for chromium oxide coating sprayed with the same equipment, and those both coatings are 5 times worse in comparison with an HVOF coating but 2 times better than hard chrome.

For industrial applications, typically finer surface is required than as-sprayed one. In the case of coatings it represents necessity of grinding of the sprayed parts. In the particular case of WSP coatings each removal of a material from the surface leads to certain opening of pores originally not connected to the surface. This factor is disadvantageous. In the other hand porosity could be utilized for a lubricant fixing at certain conditions.

4. Conclusions

To obtain the best possible WC-17Co coating with WSP process, from the viewpoint of wear resistance and hardness, the desired parameters combination is long feeding distance combined with short spray distance. It should be also recommended to have a thick enough coating and limit the cooling speed by use of less thermally conductive substrate, if possible, or by substrate preheating up to 200°C. Coating

Table 3: Comparison of the best WSP coating of WC-Co (115–300) with other materials studied by the authors under the same conditions.

MATERIAL	SAR—wear coef. [mm³/Nm]	DSRW—wear coef. [mm³/Nm]	Microhardness $HV_{0.1}$ [GPa]
WC-17Co (115–300)	0.00010	0.00017	18.67 ± 4.18
WC-17Co, HVOF	0.00002	0.00009	12.40 ± 1.16
Cr_2O_3, WSP-sprayed	0.00010	0.00113	9.62 ± 1.12
Hard chrome	0.00019	0.00056	8.84 ± 0.97

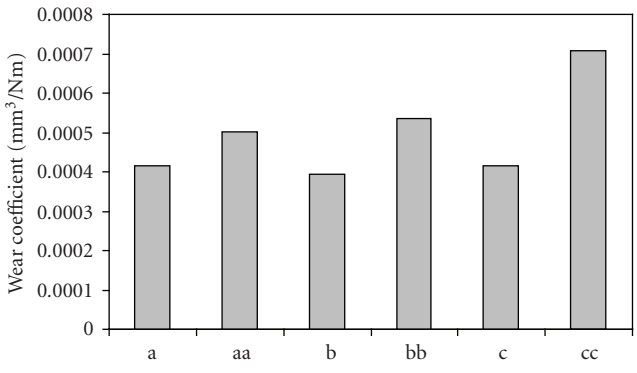

Figure 14: Results of the dry (DSRW) abrasion tests performed on (i) thick coatings on stainless steel substrates (single letter) and (ii) thin coatings on carbon steel substrates (double letter); SD 350 mm and various FD (see Table 1).

manufactured by this way is very hard but rather brittle. Despite this brittleness manifested itself in some cases by lower wear resistance than, for example, typical HVOF coatings, the WSP coatings have wear resistance comparable with hard chrome in dry and wet abrasion conditions. Interesting characteristics were found also in WC-8Co and WC-17Ni coatings, so the potential of these coatings is to be further studied. The porosity and surface roughness of all these coatings are however not as low as in other cermet coatings produced by wsp [25].

Acknowledgments

The authors acknowledge the support of the Academy of Sciences of the Czech Republic under Project CV 1QS 200430560 and they are also grateful to J. Dubsky (XRD) and B. Kolman (SEM), both of the IPP ASCR, Prague, Czech Republic.

References

[1] H. L. de Villiers Lovelock, "Powder/processing/structure relationships in WC-Co thermal spray coatings: a review of the published literature," *Journal of Thermal Spray Technology*, vol. 7, no. 3, pp. 357–373, 1998.

[2] J. Voyer and B. R. Marple, "Sliding wear behavior of high velocity oxy-fuel and high power plasma spray-processed tungsten carbide-based cermet coatings," *Wear*, vol. 225–229, part 1, pp. 135–145, 1999.

[3] D. A. Stewart, P. H. Shipway, and D. G. McCartney, "Microstructural evolution in thermally sprayed WC-Co coatings: comparison between nanocomposite and conventional starting powders," *Acta Materialia*, vol. 48, no. 7, pp. 1593–1604, 2000.

[4] P. Chraska and M. Hrabovsky, "An overview of water stabilized plasma guns and their applications," in *Thermal Spray: International Advances in Coatings Technology*, C. C. Berndt, Ed., p. 81, ASM International, Materials Park, Ohio, USA, 1992.

[5] H. Du, W. Hua, J. Liu, J. Gong, C. Sun, and L. Wen, "Influence of process variables on the qualities of detonation gun sprayed WC-Co coatings," *Materials Science and Engineering A*, vol. 408, no. 1-2, pp. 202–210, 2005.

[6] F. F. Fischer, M. D. Dvorak, and S. Siegmann, "Development of ultra thin carbide coatings for wear and corrosion resistance," in *Thermal Spray 2001: New Surfaces for a New Millennium*, C. C. Berndt, Ed., p. 1131, ASM International, Materials Park, Ohio, USA, 2001.

[7] G. Xie, J. Zhang, Y. Lu, et al., "Influence of laser treatment on the corrosion properties of plasma-sprayed Ni-coated WC coatings," *Applied Surface Science*, vol. 253, no. 23, pp. 9198–9202, 2007.

[8] H. Wang, W. Xia, and Y. Jin, "A study on abrasive resistance of Ni-based coatings with a WC hard phase," *Wear*, vol. 195, no. 1-2, pp. 47–52, 1996.

[9] O. Brandt, "The influence of HVOF parameters on microstructure and wear resistance of typical WC coatings," in *Proceedings of the 17th International SAMPE Europe Conference: Success of Materials by Combination*, pp. 391–401, Basel, Switzerland, 1996.

[10] D. A. Stewart, P. H. Shipway, and D. G. McCartney, "Influence of heat treatment on the abrasive wear behaviour of HVOF sprayed WC-Co coatings," *Surface and Coatings Technology*, vol. 105, no. 1-2, pp. 13–24, 1998.

[11] Y. Y. Santana, P. O. Renault, M. Sebastiani, et al., "Characterization and residual stresses of WC-Co thermally sprayed coatings," in *Proceedings of the 3rd International Meeting on Thermal Spraying (RIPT '07)*, L. Pawlowski, Ed., Lille, France, 2007.

[12] J.-G. Legoux, S. Bouaricha, and J. P. Sauer, "Cracking and spalling behavior of WC-17% Co cermet coatings," in *Proceedings of the International Thermal Spray Conference*, C. C. Berndt, Ed., 2006, paper no. s7_1-11196.

[13] C. Zhenda, L. L. Chewb, and Q. Ming, "Laser cladding of WC−Ni composite," *Journal of Materials Processing Technology*, vol. 62, no. 4, pp. 321–323, 1996.

[14] J. K. Knapp and H. Nitta, "Fine-particle slurry wear resistance of selected tungsten carbide thermal spray coatings," *Tribology International*, vol. 30, no. 3, pp. 225–234, 1997.

[15] "Standard test method for determination of slurry abrasivity (Miller number) and slurry abrasion response of materials

(SAR number)," Tech. Rep. ASTM: G 75–95, ASTM, Philadelphia, Pa, USA, 2002.

[16] P. Ctibor, K. Neufuss, F. Zahalka, and B. Kolman, "Plasma sprayed ceramic coatings without and with epoxy resin sealing treatment and their wear resistance," *Wear*, vol. 262, no. 9-10, pp. 1274–1280, 2007.

[17] P. Ctibor, K. Neufuss, and P. Chraska, "Microstructure and abrasion resistance of plasma sprayed titania coatings," *Journal of Thermal Spray Technology*, vol. 15, no. 4, pp. 689–694, 2006.

[18] H. Ageorges and P. Ctibor, "Comparison of the structure and wear resistance of AI_2O_3—13 wt.%TiO_2 coatings made by GSP and WSP plasma process with two different powders," *Surface and Coatings Technology*, vol. 202, no. 18, pp. 4362–4368, 2008.

[19] "Standard test method for measuring abrasion using the dry sand/rubber wheel apparatus," Tech. Rep. ASTM: G 65-00-1, ASTM, Philadelphia, Pa, USA, 2001.

[20] L. G. Yu, K. A. Khor, H. Li, K. C. Pay, T. H. Yip, and P. Cheang, "Restoring WC in plasma sprayed WC-Co coatings through spark plasma sintering (SPS)," *Surface and Coatings Technology*, vol. 182, no. 2-3, pp. 308–317, 2004.

[21] G. Xie, X. Lin, K. Wang, X. Mo, D. Zhang, and P. Lin, "Corrosion characteristics of plasma-sprayed Ni-coated WC coatings comparison with different post-treatment," *Corrosion Science*, vol. 49, no. 2, pp. 662–671, 2007.

[22] C. N. Machio, G. Akdogan, M. J. Witcomb, and S. Luyckx, "Performance of WC-VC-Co thermal spray coatings in abrasion and slurry erosion tests," *Wear*, vol. 258, no. 1–4, pp. 434–442, 2005.

[23] J. B. J. W. Hegeman, J. Th. M. de Hosson, and G. de With, "Grinding of WC-Co hardmetals," *Wear*, vol. 248, no. 1-2, pp. 187–196, 2001.

[24] P. Fauchais, M. Fukumoto, A. Vardelle, and M. Vardelle, "Knowledge concerning splat formation: an invited review," *Journal of Thermal Spray Technology*, vol. 13, no. 3, pp. 337–360, 2004.

[25] P. Ctibor, H. Ageorges, K. Neufuss, and F. Zahalka, "Composite coatings of alumina-based ceramics and stainless steel manufactured by plasma spraying," *Medziagotyra*, vol. 15, no. 2, pp. 108–114, 2009.